

Received December 9, 2016, accepted December 26, 2016, date of publication January 26, 2017, date of current version March 2, 2017.

Digital Object Identifier 10.1109/ACCESS.2017.2647817

Robust and Reliable Predictive Routing Strategy for Flying Ad-Hoc Networks

GANBAYAR GANKHUYAG, ANISH PRASAD SHRESTHA, AND SANG-JO YOO

Department of Information and Communication Engineering, Inha University, Incheon 402-751, South Korea

Corresponding author: S.-J. Yoo (sjyoo@inha.ac.kr)

This work was supported in part by the Basic Science Research Program through the National Research Foundation of Korea under Grant NRF-2014R1A2A2A01002013 and in part by Information Technology Research Center support program IITP-2016-H8501-16-1019 supervised by the Institute for Information and communications Technology Promotion by the Ministry of Science, ICT and Future Planning.

ABSTRACT Ever-increasing demands for portable and flexible communications have led to rapid growth in networking between unmanned aerial vehicles often referred to as flying ad-hoc networks (FANETs). Existing mobile *ad hoc* routing protocols are not suitable for FANETs due to high-speed mobility, environmental conditions, and terrain structures. In order to overcome such obstacles, we propose a combined omnidirectional and directional transmission scheme, together with dynamic angle adjustment. Our proposed scheme features hybrid use of unicasting and geocasting routing using location and trajectory information. The prediction of intermediate node location using 3-D estimation and directional transmission toward the predicted location, enabling a longer transmission range, allows keeping track of a changing topology, which ensures the robustness of our protocol. In addition, the reduction in path re-establishment and service disruption time to increase the path lifetime and successful packet transmissions ensures the reliability of our proposed strategy. Simulation results verify that our proposed scheme could significantly increase the performance of flying ad hoc networks.

INDEX TERMS FANET, routing protocol, directional transmission, route setup, average path lifetime, dynamic angle adjustment.

I. INTRODUCTION

The fast-growing global industry of the unmanned aerial vehicle (UAV), commonly known as the drone, has already found application in both civil and military-operations such as real-time surveillance [1], wildfire monitoring [2], search and rescue operations [3], reconnaissance operations, hazardous site inspection [4], range extension and the agriculture field [5]. A typical UAV may operate with various degrees of autonomy: either remote control by infrastructure such as a ground base and satellite, or via fully autonomous onboard computer. In order to avoid the restrictions introduced by the infrastructure-based communications architecture, ad-hoc networking between UAVs is preferred. This created a new paradigm, referred to as the flying ad-hoc networks (FANETS) where each flying UAV can act as a router [6].

FANETs are not only resilient against isolated attacks or node failure, but they are also relatively economical. As FANET nodes operate in the sky, line-of-sight communications is possible most of the time. Moreover, it can be

rapidly deployed for real-time communications anywhere, as these networks do not rely on any external support. Although such features make FANETs an appropriate solution in several application scenarios, they also bring challenging communications and networking problems [7], [8]. Despite its similarity to the mobile ad-hoc network (MANET) and to the vehicular ad-hoc network (VANET) in terms of peer-to-peer communications, the FANET is characterized by certain unique features. The speed of a typical UAV in FANET ranges from 30 – 460 km/h with movement in three-dimensional space. As such, the network topology keeps changing [9] and the distance between flying nodes will be long, resulting in loss of connections. This will disrupt the flow of data packets in already established routing path. Long-distance communications also consume a lot of power which can make a lightweight UAV with limited battery power infeasible. Since FANETs are deployed for sensitive military and monitoring applications that demand guaranteed data delivery with low latency, reliability, and robustness, quick route setup must also be taken into account. Under these

circumstances, designing a routing protocol is quite challenging in FANETs.

Motivated by these facts, we propose a *robust and reliable predictive* (RARP) routing protocol based on three-dimensional estimation with a fast update mechanism for the flying path in FANETs. The main features and contributions of this paper can be summarized as follows:

- 1) We derive the closed form expression to measure expected connection time between two adjacent intermediate nodes with directional transmission in three dimension using predictive approach.
- 2) Based on fresh trajectory and location information, we use directional beamforming once the route request (RREQ) is received at the destination. This not only increases the transmission distance but also shortens the route setup time and reduces packet collisions.
- 3) We allow each packet to piggyback current position and speed information to update the flying path and improve prediction accuracy.
- 4) We introduce dynamic angle adjustment to avoid the *near* and *far* node problems during directional transmission which extends the average path lifetime.
- 5) Based on the estimated expiry time of the current established path, we setup an alternative path to reduce service disruption time. This alternative path can be setup simultaneously with the data transmission process.
- 6) We allow the transmitting node to switch back to omnidirectional transmission if it is unable to receive acknowledgement for a predetermined number of trials. If the transmitting node can receive acknowledgement, it can update the information about the receiver and again switch back to directional transmission. This allows local repair of the routing path.

The rest of this paper is organized as follows. Related works are presented in Section II. In Section III, we present the proposed routing scheme and its features in detail. The performance evaluation of the proposed protocol is presented in terms of route setup success rate, average path lifetime, successful data transmission rate and service disruption time, with simulation results in Section IV. Conclusions are drawn in Section V.

II. RELATED WORKS

Traditional routing protocols often use omnidirectional transmission which causes lots of collisions and severely limits the transmission range. Directional antennas are often utilized to overcome such problems. Use of a directional antenna was studied by Temel and Bekmezci [12] to design a medium access control (MAC) protocol for FANETs. The authors aimed to increase spatial reuse as well as overall network capacity while addressing the deafness problem of directional MAC. However, the issues related to routing protocol were not addressed by the authors. Most of the routing protocols designed for MANETs and VANETs such as ad-hoc on-demand distance vector (AODV) and optimized link-state

routing (OLSR) along with its variants simply fail to track the fast changes in topology of a FANET [10], [11].

In recent years, a handful of alternative schemes have been proposed to address rapid changes in network topology. Vasiliev et. al [13], proposed simple packet delivery ratio as an evaluation metric to compare quality of service in contention-based, greedy, and predictive approaches to peer selection. Insights into the workings of an actual routing protocol were not presented. A bee algorithm inspired by the bee-hive operating principle based on a clear distribution of responsibilities among the bees was proposed by Leonov [14]. A major drawback in this technique is the long end-to-end delays which may pose serious barrier to FANET implementation. Similarly, ant colony optimization (ACO) was presented by Maistrenko et al. [15] based on the metaheuristic swarm method for the solution to combinatorial optimization polynomial tasks in a graph model. Although ACO has relatively short end-to-end delay, overhead costs are quite high. The application of OLSR and predictive OLSR was proposed by Singh and Verma [10] and Rosati et. al [16] respectively. OLSR technique uses multi-point-relay (MPR) to reduce network traffic and flooding in the network, whereas the proposed predictive OLSR also takes advantage of information from global positioning information, and finds a route based on expected transmission count and speed. A major concern in OLSR is that it requires relatively more storage complexity and usage, along with frequent transmission of control packets, like the *Hello* message. The number of MPRs is also crucial in design issues that affect delay significantly. Another downside to OLSR is that it must maintain information about routes that may never be used, hence wasting possibly scarce resources. Besides these facts, other important parameters to evaluate the routing protocol, such as route setup success rate, average pathlife time, successful data delivery, the effects of the mobility model, and service disruption time are also not jointly investigated in any of the above studies.

On a different note, although existing AODV-based schemes cannot directly address the requirements of FANET, the FANET is adaptive to vigorous link conditions, and needs few control packets and little memory overhead to find unicast paths to destinations nodes in the ad hoc network. It forms route only for those nodes that are requested by the source node according to its need, and keeps the route until it is required by the source node. Unlike the aforementioned works, our proposed RARP routing protocol introduces several new features to improve the conventional AODV scheme making it suitable for FANETs. We present not only joint study of essential parameters like route setup success rate, average pathlife time etc., but also focus on increasing robustness and reliability of the established routing path itself.

III. PROPOSED RARP ROUTING SCHEME

We assume that all flying nodes are equipped with a global positioning system (GPS) and the i -th node has a

three-dimensional position $\{x_i, y_i, z_i\}$, movement vector i.e. velocity $\{v_{x,i}, v_{y,i}, v_{z,i}\}$ and flying risk r_i . The flying risk accounts for the failure probability of a node which is based on two types of parameters. The first one is node specific such as stored energy, size, maneuvering skills, operation requirements and mission updates. The second one is based on geographic location such as environmental conditions and terrain structures such as wind, rain, humidity, atmospheric pressure, tall buildings, mountains etc. The following subsection provides an in-depth explanation of each new feature of our proposed RARP routing scheme.

TABLE 1. Modified RREQ format.

Parameters	Symbols
Route to find	$S_{id} - D_{id}$
RREQ request time	t_{RREQ}
RREQ sender ID	id
Sender's location	$\{x, y, z\}$
Sender's movement vector	$\{v_x, v_y, v_z\}$
Hop count	Hop_{count}
Maximum risk value	$max R$
Minimum expected connection time	$min CT$

A. PREDICTION OF EXPECTED CONNECTION TIME

Unlike the conventional RREQ format in AODV, the modified RREQ in our proposed scheme includes trajectory information about the sender's three-dimensional location, movement vector, minimum expected connection time of the RREQ path, and maximum risk value. A source node that wants to find a path to the destination node broadcasts an RREQ packet using omnidirectional transmission to the neighboring nodes. Any intermediate node that receives the RREQ packet rebroadcasts it until the packet reaches the destination. Table 1 shows the format of the modified RREQ packet. When a node receives the RREQ packet, it can calculate the maximum risk and the expected connection time between the RREQ sender and receiver using both of the UAV's information. For instance, we consider two nodes n_i and n_j , at time t_0 separated by distance $d_{i,j}(t_0)$ as shown in Fig. 1, where the value of $d_{i,j}(t_0)$ can be computed as

$$d_{i,j}(t_0) = \sqrt{(x_j - x_i)^2 + (y_j - y_i)^2 + (z_j - z_i)^2}. \quad (1)$$

As time passes, the movement of nodes creates further separation between these two respective nodes. At a certain point in time (say t_3 s.t. $t_3 = t_0 + t$), distance between nodes reaches $d_{i,j}(t_0 + t)$ such that $d_{i,j}(t_0 + t) = d_{max}$ where d_{max} is the maximum distance that can be offered by directional transmission given by

$$d_{max} = \sqrt{\beta \frac{G_r G_t \lambda^2 P_t}{2\pi \theta P_r^{min}}}, \quad (2)$$

where G_r is the receiving antenna gain, G_t is the transmitting antenna gain, λ is signal wavelength, P_t is predetermined omnidirectional transmission power, P_r^{min} is minimum decodable power, β is the pathloss exponent and θ is the angle of the directional antenna. Since the flying nodes usually have

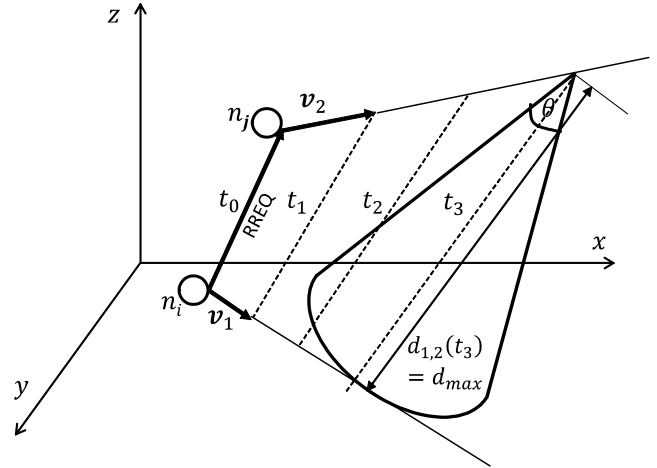


FIGURE 1. Minimum expected connection time calculation.

forward motion and require minimum turning radius, we can assume that both nodes have the same velocity at time t_3 as in time t_0 . As such, the expression for $d_{i,j}(t_0 + t)$ can be obtained as

$$d_{i,j}(t_0 + t) = \sqrt{\begin{aligned} &((x_j + v_{x,j}t) - (x_i + v_{x,i}t))^2 \\ &+ ((y_j + v_{y,j}t) - (y_i + v_{y,i}t))^2 \\ &+ ((z_j + v_{z,j}t) - (z_i + v_{z,i}t))^2. \end{aligned}} \quad (3)$$

Any further separation beyond distance d_{max} will finally cause loss of the connection between these two nodes. As such, the expected connection time can be obtained as

$$t_{i,j}^{ct} = (t_3 - t_0). \quad (4)$$

In other words, the expected connection time (CT) is the time duration until the distance between the two nodes reaches d_{max} . Nonetheless, the expression for the expected connection time in terms of position and speed can be solved by $d_{i,j}(t_0 + t_3) = d_{max}$. Hence, the final expression of the expected connection time can be obtained by solving the quadratic equation for t given below

$$\begin{aligned} &(V_{xd}^2 + V_{yd}^2 + V_{zd}^2)t^2 + 2(X_d V_{xd} + Y_d V_{yd} \\ &+ Z_d V_{zd})t + (X_d^2 + Y_d^2 + Z_d^2 - d_{max}^2) = 0 \end{aligned} \quad (5)$$

where $X_d = x_j - x_i$, $Y_d = y_j - y_i$, $Z_d = z_j - z_i$, $V_{xd} = v_{x,j} - v_{x,i}$, $V_{yd} = v_{y,j} - v_{y,i}$, $V_{zd} = v_{z,j} - v_{z,i}$.

When an intermediate node rebroadcasts the RREQ packet, it replaces the sender's ID, sender's location, sender's movement vector in its information as shown in Table 1. The hop count is incremented by 1, implying the addition of a single hop. Similarly, max_R and min_{CT} indicate the maximum risk and minimum expected connection time of the path that the RREQ packet traversed from the source to the current intermediate node. For instance, if we assume that total hop count at the current intermediate node is N_H , the minimum expected connection time can be obtained as

$$\min CT = \min \{t_{1,2}^{ct}, t_{2,3}^{ct}, \dots, t_{N_H, N_{H+1}}^{ct}\}. \quad (6)$$

TABLE 2. Modified backward table.

Node j 's backward table			
Route	$S_{id} \rightarrow D_{id}$	Previous node	i
Previous node position	$\{x_i, y_i, z_i\}$	Previous node speed	$\{v_{x,i}, v_{y,i}, v_{z,i}\}$
Position update time	t_0		
Utility	U		

Similarly, the maximum risk can be obtained as

$$\max R = \max \{r_1, r_2, \dots, R_{N_{H+1}}\}. \quad (7)$$

B. UTILITY FUNCTION FOR PATH SELECTION

Whenever an intermediate node j receives an RREQ, if it is not the destination or it does not have the route information to the destination, then it builds a backward table as shown in Table 2. Besides information about the previous node position, the movement vector and the update time, the backward table also stores the value of the utility function given by

$$U = \omega_{CT} \times \min CT - \omega_H \times Hop_{count} - \omega_R \times \max R \quad (8)$$

where ω_{CT} , ω_H , and ω_R represent the corresponding weights for $\min CT$, Hop_{count} , and $\max R$, respectively such that $\omega_{CT} + \omega_H + \omega_R = 1$.

However, if intermediate node j receives the RREQ more than once, it would have already built up the backward table. In this case, information in the new RREQ packet. If the new utility value is greater than in the existing backward table it will compute the utility function using, then it is replaced with the new RREQ information. As such, intermediate node j updates the RREQ packet with following changes

- 1) If $r_j > \max R \rightarrow \max R = r_j$,
- 2) If $t_{i,j}^{ct} < \min CT \rightarrow \min CT = t_{i,j}^{ct}$, and
- 3) $Hop_{count} = Hop_{count} + 1$.

The updated RREQ is then rebroadcasted. Since the utility function in (8) is composed of weighted expected connection time, hop count and risk value, selected routing path will properly balance between the expected connection time, number of hops and node failure probability. It should be remembered that the routing path with longer expected connection time will help to increase lifetime of the path, fewer number of hops can reduce delay, and lower node failure probability will ensure that that the nodes are less susceptible to breakdown. Therefore, negative signs are used for maximum of hop count and risk value, while positive sign for minimum of connection time. Furthermore, the value of connection time and hop count is not bounded within 0 and 1, while risk is bounded as $0 \leq R \leq 1$. Since $\omega_{CT} + \omega_H + \omega_R = 1$, we normalized the connection time and number of hops to approximately bound them between 0 and 1. For instance, $\min CT$ can be normalized by scaled version of maximum possible connection time which can be obtained from (5) and number of hops can be normalized by scaled

TABLE 3. Modified RREP format.

Parameters	Symbols
Route to find	$S_{id} - D_{id}$
RREQ request time	t_{RREQ}
Minimum expected connection time	$\min CT$
RREP sender ID	id
Destination's location	$\{x, y, z\}$
Destination's movement vector	$\{v_x, v_y, v_z\}$
Destination's RREP response time	t_{RREP}
Sender's location	$\{x, y, z\}$
Movement vector	$\{v_x, v_y, v_z\}$

version of maximum possible hop count. Note that maximum possible hop count is $N - 1$ where N is number of nodes.

C. DIRECTIONAL TRANSMISSION WITH UPDATE MECHANISM

Once the RREQ is received by the destination node, it will wait for a certain amount of time. If it receives multiple RREQ, it selects the optimum path based on the utility function as derived in (8). Then, the destination node will respond by unicasting the modified route reply (RREP) as shown in Table 3. The RREQ request time and final $\min CT$ of the RREP is not changed by any intermediate nodes while the RREP sender's location and movement vector information is replaced by other intermediate nodes before they forward the packet. Destination node information is used for the path re-initialization step, which is covered in Section III-E.

Using the backward table to the source node, intermediate nodes can determine which node the packet should be sent to next. Since the RREP sending node is aware of the past position and movement of its intended receiver, it can estimate the location at time t as

$$\begin{aligned} x_{j,est} &= x_j + v_{x,j}(t - t_0), \\ y_{j,est} &= y_j + v_{y,j}(t - t_0), \\ z_{j,est} &= z_j + v_{z,j}(t - t_0). \end{aligned} \quad (9)$$

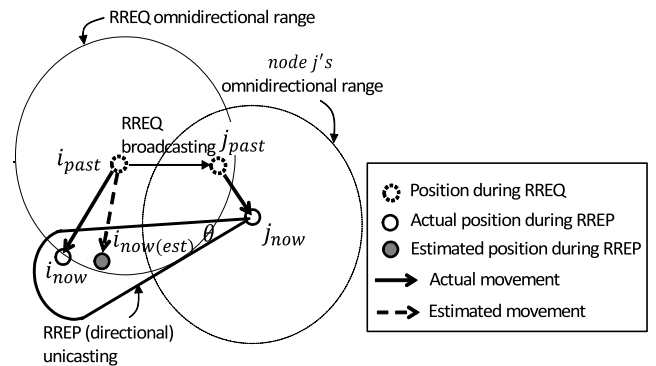


FIGURE 2. Directional RREP transmission towards estimated position.

After computing an estimation of the current location of the intended receiver, RREP packet can be transmitted using the directional antenna by beamforming towards the estimated position with angle θ shown in Fig. 2. Under constant transmission power, the directional antenna will have

longer transmission distance than a typical omni-directional antenna. Consequently, the connectivity in the FANET will be increased.

TABLE 4. Modified forward table.

Node i 's forward table			
Route	$S_{id} \rightarrow D_{id}$	Previous node	j
Previous node position	$\{x_j, y_j, z_j\}$	Previous node speed	$\{v_{x,j}, v_{y,j}, v_{z,j}\}$
Position update time	t_0		

When a node receives an RREP packet, it stores the RREP sender's information in its forward table as shown in Table 4. After the RREP packet reaches the source node, DATA packet transmission starts. During DATA transmission, the beam-forming antenna automatically changes the directionality of its radiation patterns to the next node on the path towards the destination based on the forward table information. During DATA transmission, sender i (source or intermediate nodes) piggybacks its position and movement vector onto the DATA packet. Furthermore, the receiving node updates its backward table for node i based on the piggybacked information in the DATA packet. Likewise, after receiving a DATA packet, the receiving intermediate node j will also piggyback its current position and movement vector onto the acknowledgement (ACK) packet, as shown in Fig. 3. If the intermediate node i receives the ACK, it will update its forward table for node j . By exchanging DATA and ACK packets with piggybacked information, the related fresh location and movement vector information of the peer node can be maintained. Such a fresh update mechanism will constantly maintain the accuracy of our prediction mechanism.

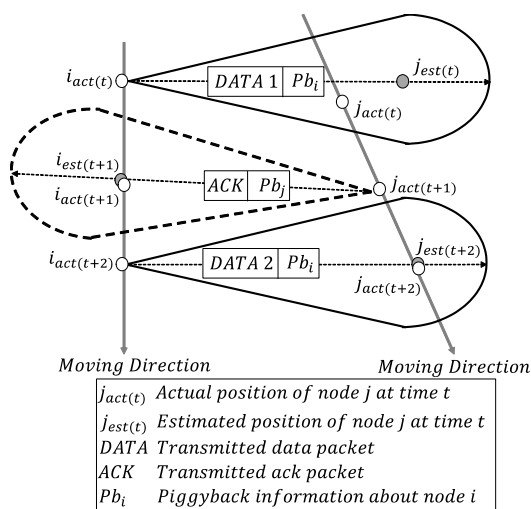


FIGURE 3. Update mechanism during DATA and ACK transmission.

D. DYNAMIC ANGLE ADJUSTMENT

Our proposed scheme predicts the approximate position of the receiver based on backward and forward tables, assuming

the movement vector remains the same as in those tables during the time of prediction. At the time of DATA or ACK transmission, the main lobe of radiated power is concentrated towards the estimated position. However, if the movement vector of the receiver has already been changed before the time of prediction, the estimated and actual positions of the receiving node will be different, resulting in error. If the actual position is outside the coverage area of directional transmission, it will cause a loss of connection. In order to avoid such situations, we tackle two specific problems which we refer as the *near node problem* and the *far node problem*.

It should be noted that the smaller the value of θ , the longer the propagation area with a narrow beamwidth, whereas the higher the value of θ , the shorter will be the propagation area with a wide beamwidth. As such, a near node problem occurs when the estimated receiving node is quite near to the transmitting node and the angle is small. As shown in Fig. 4, for the same estimation error, if the estimated distance is short and the angle is small, then the success probability for coverage can decrease. To solve the near node problem, we need to use a wider angle. On the other hand, the far node problem occurs when the distance between transmitting and receiving node positions is nearly equal to the maximum distance offered by the current angle value. In order to overcome the far node problem, we need to use a narrow angle so the transmission distance can be increased. Hence, dynamic adjustment of the angle is required to tackle these two problems.

Under the fixed transmission power condition, the propagation area and maximum transmission distance can be determined for corresponding directional antenna angles. For N possible angles $\theta_1, \theta_2, \dots, \theta_{N-1}, \theta_N$, we can determine N corresponding maximum transmission distances, $d_{max1}, d_{max2}, \dots, d_{maxN-1}, d_{maxN}$. As such, we can dynamically adjust the directional antenna angle according to the estimated distance ($d_{i,j}$), between the DATA or ACK sending node position and estimated receiving node position. Since the intended receiver can move in either direction, instead of using an exact value of the estimated distance for angle adjustment, we introduce certain guard factor α such that $0 < \alpha < 1$. The value of α is basically dependent on the speed of flying node. Higher the value of α , higher is the value of α and vice versa. Finally, the directional antenna angle can be dynamically adjusted based of the value of guard factor α and $d_{i,j}$ as shown in Table 5. This can overcome the near and far problems ensuring robustness of the proposed protocol. In practice, dynamic angle adjustment can be implemented by using an *adaptive antenna*.

E. ALTERNATIVE PATH SETUP

In our proposed protocol, we are aware of the minimum expected connection time between two adjunct intermediate nodes of the selected path. This can provide a rough estimation of the routing path lifetime. Therefore, we intend to proactively setup an alternative path before the minimum expected connection time expires. During the route discovery process, when the source node receives the RREP at time t ,

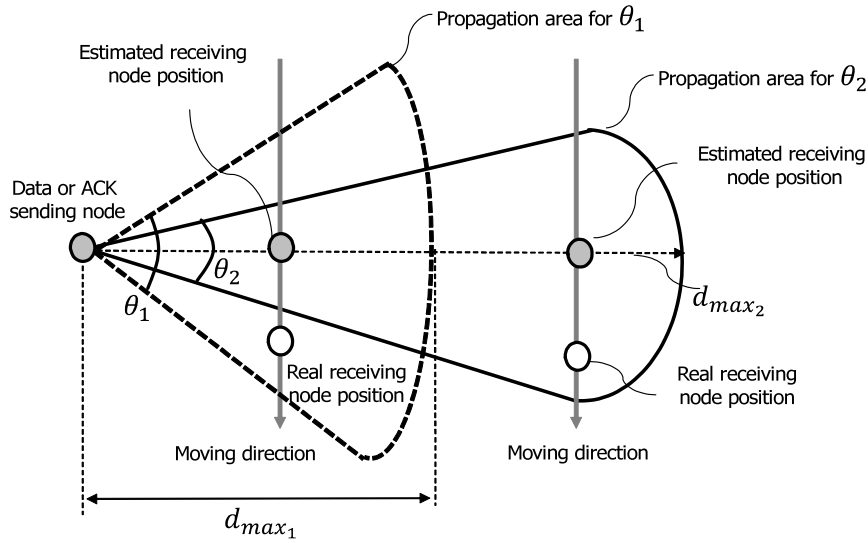


FIGURE 4. Near node problem.

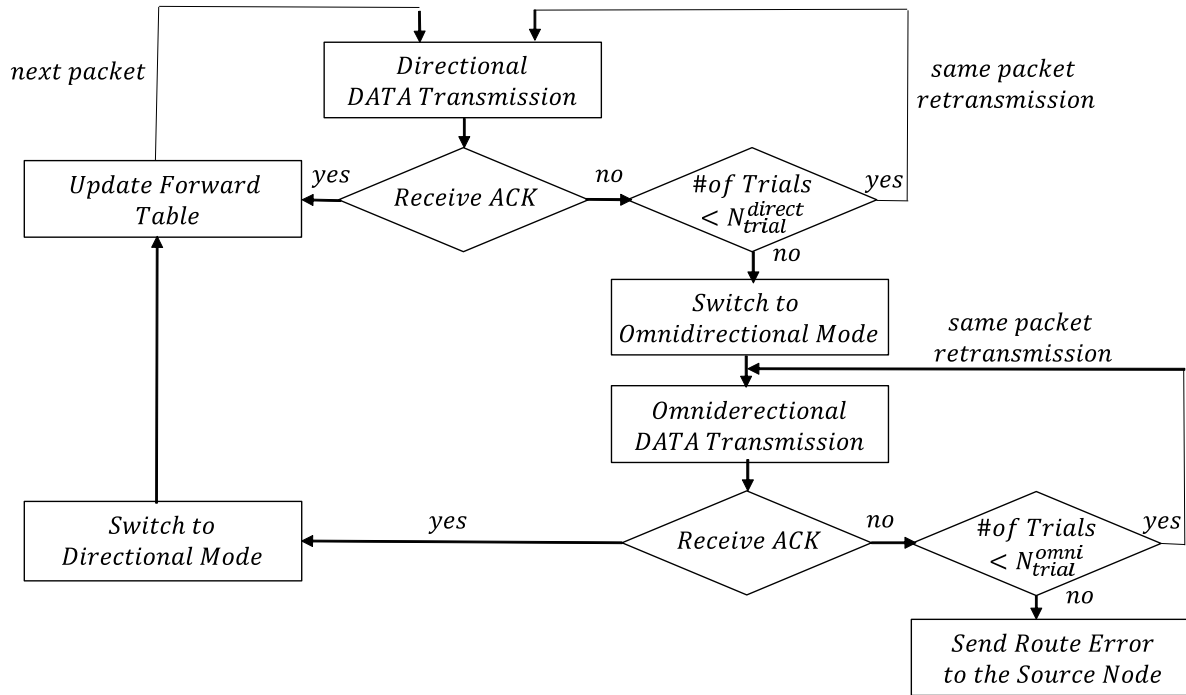


FIGURE 5. Flowchart depicting local path repair.

we set route re-initialization timer T_{route} using t_{RREQ} and min CT of the RREQ as shown below:

$$T_{route} = (t - t_{RREQ} + \min CT) \times \Psi \quad (10)$$

where $\Psi < 1$. After countdown timer T_{route} reaches zero, the source node starts the route re-initialization. The value of Ψ signifies how early the route re-initialization process starts before the expiry of the minimum expected connection time. Since the source node has a rough estimate for the position of the destination, the re-initialization RREQ can be broadcasted

with a large direction angle antenna (θ_{re}) instead of an omnidirectional angle. For example the value of θ_{re} can be π . If the current routing path exists till the minimum expected connection time, the route re-initialization process can be performed simultaneously with DATA packet transmission. The availability of an alternative routing path in such a scenario will totally avoid any service disruption. On the other hand, if the routing path does not exist till the minimum expected connection time, then proactive route re-initialization with a directional antenna will reduce the service disruption-time.

TABLE 5. Angle adjustment based on estimated distance.

Condition	Directional antenna angle
$0 \leq d_{i,j} \leq (\alpha \times d_{max1})$	θ_1
$(\alpha \times d_{max1}) \leq d_{i,j} \leq (\alpha \times d_{max2})$	θ_2
\vdots	\vdots
$(\alpha \times d_{max_{N-2}}) \leq d_{i,j} \leq (\alpha \times d_{max_{N-1}})$	θ_{N-1}
$(\alpha \times d_{max_{N-1}}) \leq d_{i,j}$	θ_N

F. LOCAL PATH REPAIR

Although a fresh update mechanism with piggybacked information in DATA and ACK packets as well as a dynamic directional angle adjustment can capture the erratic behavior of high-speed flying nodes, it cannot guarantee the maintenance of a connection all the time. To address such a problem, we design a local path repair technique as shown in Fig. 5. After a predetermined number of directional transmissions say N_{trial}^{direct} , if a node still fails to receive ACK, then it switches to omnidirectional transmission mode in order to cover more area. The node is then allowed to transmit the same DATA packet for another N_{trial}^{omni} times. If the node receives ACK within N_{trial}^{omni} trials, it can update the forward table with a new position and movement vector. For the next data transmission, the node can again switch back to directional DATA transmission to beamform towards the new estimated location. However, if the node fails to receive ACK for the predetermined number of omnidirectional DATA retransmissions, then the node sends a route error message to the source node. Afterwards, the source node starts the route-initialization procedure.

TABLE 6. Simulation parameters.

Parameters	Value
Simulation time	100 sec
Simulation space	$5 \times 5 \times 2 (Km^3)$
Omnidirectional transmission power (P_t)	1000 mW
Minimum decodable power (P_r^{min})	-70 dBm
Pathloss exponent (β)	2
Frequency	2.4 GHz
Non adaptive antenna angle (θ)	90
Adaptive antenna angle (θ)	90, 135, 210, 360
Unit time	20 msec
Data transmission rate	10 – 200
Keep time	5 – 50 sec

IV. SIMULATION RESULTS

In this section, we investigate the performance evaluation of our proposed routing strategy in terms of route setup success, average path lifetime, data delivery ratio and service disruption time. We compare the proposed scheme with a conventional AODV scheme using an omnidirectional antenna as it is often used for benchmark comparison [19], [20]. We use C++ to perform Monte Carlo simulations. The simulation environment parameters are presented in Table 6. We assume different types of flying nodes are deployed at different geographic locations within the simulation space. In order to capture the failure probability of each node introduced by geographic

location and node specific constraints, we initialize risk value of all the nodes accordingly ranging between 0 and 1. In other words, the risk value of each flying node differs based on its type and location. Note that the angle for the proposed scheme with non-adaptive antenna is 90 while the proposed scheme with an adaptive antenna can select from a set of four angles (90°, 135°, 210°, and 360°) throughout the simulation unless otherwise stated. We adopt the random waypoint mobility model to capture the random movement of nodes such that it can mimic the movement of a flying UAV. The flying node moves in one direction at a certain speed for a period of time, which we refer to as keep time from hereon. After the current keep time, the node then randomly chooses a new direction with a different velocity and keep time. Since the flying node does not suddenly move in a backward direction or make sharp turns, that should be taken into account when choosing a new direction and speed. We refer to the time required for one-hop communications as a unit time and to the message transmission interval by the source node as the data transmission rate. Thus, a message transmission interval of 10 with a unit time of 20 msec implies that the message is transmitted at intervals of 200 msec.

At first, we examine the route setup success rate, which represents successful reception of RREP at the source node from the RREQ packet transmission. Fig. 6 shows the route setup success rate against several parameters such as the number of nodes, the speed, the directional antenna angle and the keep time. It is easily seen that success rate increases with an increase in the number of nodes for both the proposed and the conventional scheme, because more nodes usually increases the probability of the existence of several intermediate nodes between source and destination. However, the route setup success rate is always higher for the proposed scheme compared to the conventional scheme irrespective of the number of nodes. The contributing factor behind such an improvement in performance can be attributed to directional beamforming towards the estimated location of the RREP receiver. On the other hand, although the same amount of RREQ packets are received at the destination node under the conventional scheme, it is unable to send back RREP packets in a similar fashion like our proposed scheme because the intermediate nodes are selected solely on the number of hop counts. We also observe that the success rate for the proposed scheme remains unaffected by an increase in speed whereas the conventional scheme degrades with an increase in speed for the same reason mentioned earlier. A similar improvement in route setup success rate was noticed for our proposed scheme, in terms of directional antenna angle and keep times. It should be noted that a successful route setup usually takes a relatively short span of time. Therefore, a change in angle or keep time does not influence the route setup success rate performance of either schemes.

In Fig. 7, we examine the average path lifetime of the conventional scheme and the proposed scheme against several parameters as in Fig. 6. In Fig. 7 (a), it is easily seen that a directional transmission scheme with predictive location

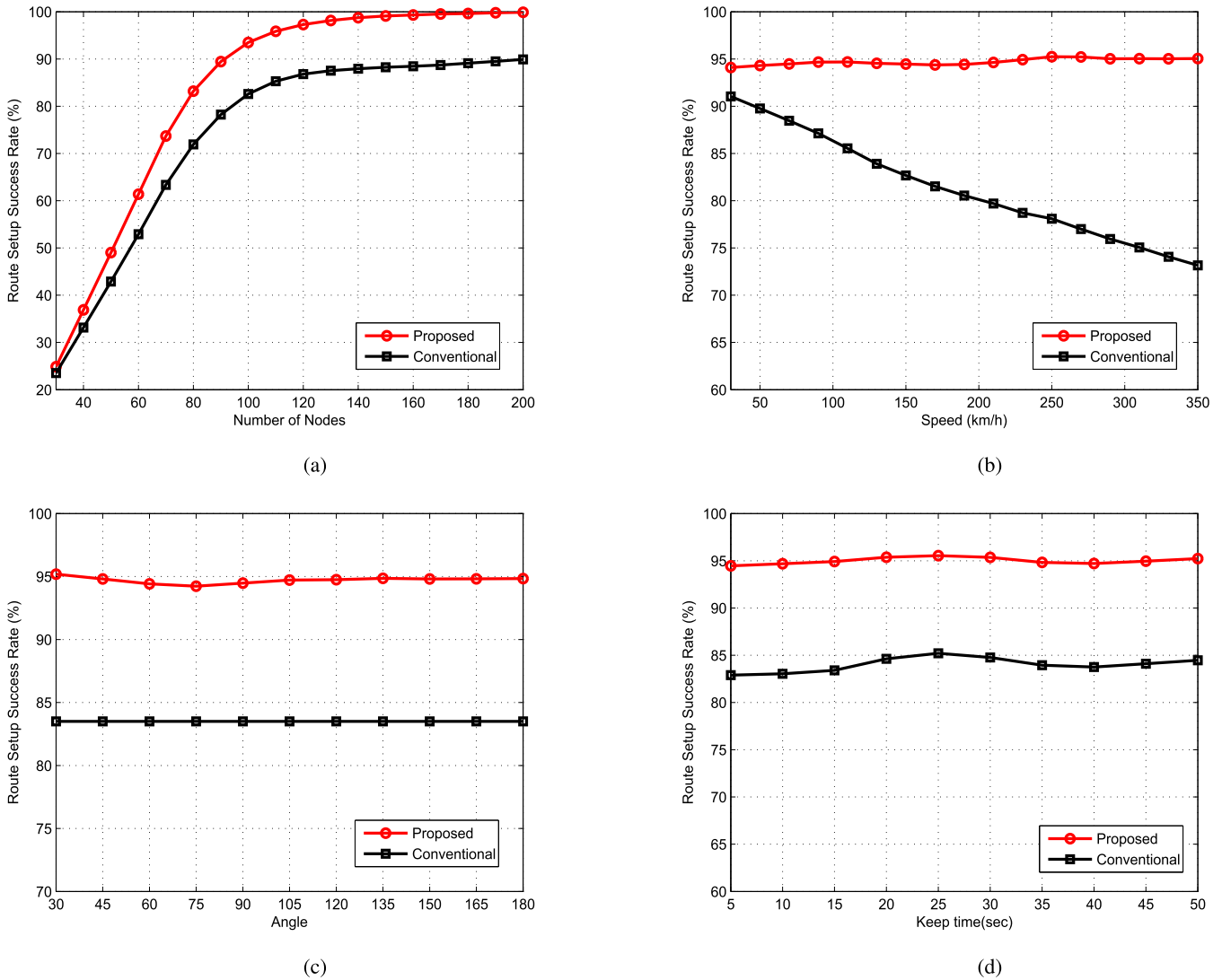


FIGURE 6. Route setup success rate vs. (a) number of nodes (speed = 140~160 km/h and keep time = 10 sec), (b) speed (number of nodes = 100 and keep time = 10 sec), (c) angle (number of nodes = 100, speed = 140~160 km/h, keep time = 10 sec), and (d) keep time (number of nodes = 100, speed = 140~160 km/h).

estimation can significantly increase the average path lifetime in comparison to the conventional one. As the value of θ increases, the transmission range decreases and the proposed scheme is unable to take full advantage of three-dimensional location estimation; performance degrades to the same degree as in the omnidirectional case. In Figs. 7 (b), (c) and (d), we examine the average path lifetime of the conventional scheme and our proposed directional transmission scheme with and without dynamic angle adjustment. For the transmission scheme without angle adjustment, we arbitrarily assign $\theta = 90$ which offers a transmission distance of approximately 2 km based on the above the simulation parameters. Similarly, for the transmission scheme with angle adjustment, $\theta \in \{90, 135, 210, 360\}$ so that the maximum offered transmission distance is approximately 2 km and minimum offered transmission distance is same as that of omnidirectional transmission scheme which is approximately 1 km in this case.

The option of multiple antennas allows setting multiple transmission range with appropriate beamwidths. We can easily see that both adaptive and non-adaptive antenna scheme provides sufficiently longer path lifetime, compared to the conventional omnidirectional scheme. We can also see that the adaptive antenna scheme provides slightly more improvement than the non adaptive antenna scheme as it can tackle the near node and far node problem reducing the estimation error. Note that although fewer nodes results in a low path setup success rate, the path lifetime is almost independent of the number of nodes. Even when the number of nodes is few, path lifetime is quite high. This is because once the path is set up, we constantly update the location information in backward and forward tables during DATA and ACK transmission which maintains the accuracy of the prediction mechanism. On the other hand, although average path lifetime decreases with increase in speed, the performance gap between the

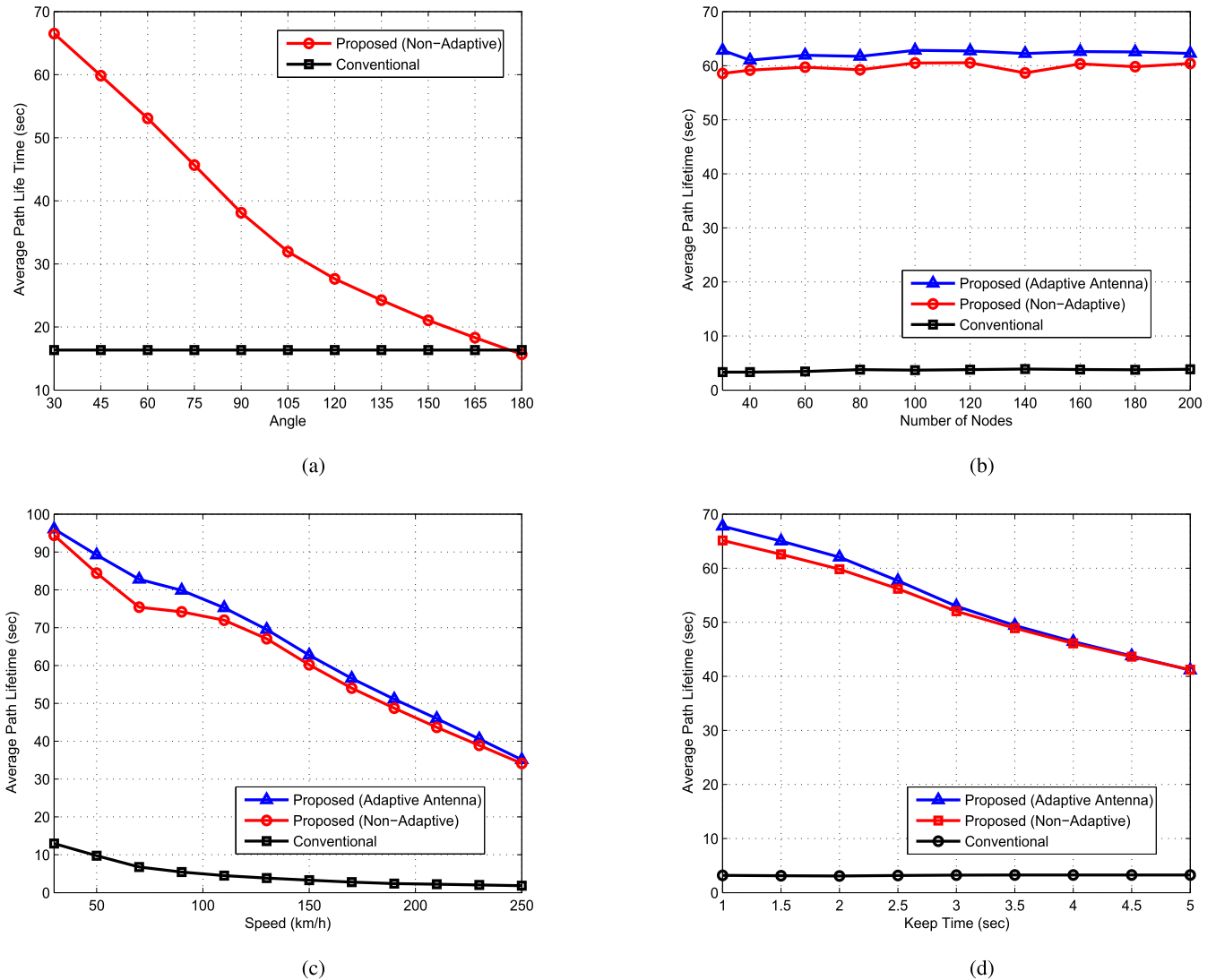


FIGURE 7. Average path lifetime vs. (a) angle (number of nodes = 100, speed = 140~160 km/h, keep time = 10 sec), (b) number of nodes (speed = 140~160 km/h, keep time = 10 sec), (c) speed (number of nodes = 100, keep time = 10 sec), and (d) keep time (number of nodes = 100, speed = 140~160 km/h).

proposed scheme and the conventional scheme remains quite high. This is because we can exploit the extra transmission distance offered by directional antenna in comparison to the omni-directional antenna. Moreover, the parameters set in the mobility model may differ based on the size and nature of the flying UAV. To capture this effect, we investigate the average path lifetime against keep time in Fig. 7(c). We can see this if the keep time increases i.e. the flying node moves in one direction for a long time without a change in direction. If any two neighboring intermediate UAVs on the path continue to fly away from each other, then the link will be disconnected within a relatively short time. However, when the keep time is small UAVs frequently change their directions, so that the actual average path lifetime can be extended. As such, the average lifetime decreases with increase in keep time.

Fig. 8 illustrates a comparison of hop counts between the proposed and conventional scheme. We set $\omega_{CT} = \omega_H =$

$\omega_R = 0.33$ to obtain the utility function value for the proposed scheme. We can see that hop count increases until the number of node reaches 60 and remains identical for both schemes. When the number of node goes beyond 60, hop count decreases for the conventional scheme, whereas it tends to approximately saturate under the proposed scheme. It was found that under the given simulation parameters, not all nodes can be fully connected until the number of nodes reach around 60. Therefore, hop count increase in a similar fashion for both schemes until the number of node reached 60. Beyond this value, nodes are fully connected and since the conventional scheme selects a path with the minimum number of hops while selecting intermediate nodes, we find that hop count decreases. But, in the proposed scheme, risk and connection time are also considered, besides the number of hops, so we can see an insignificant increment in hop count.

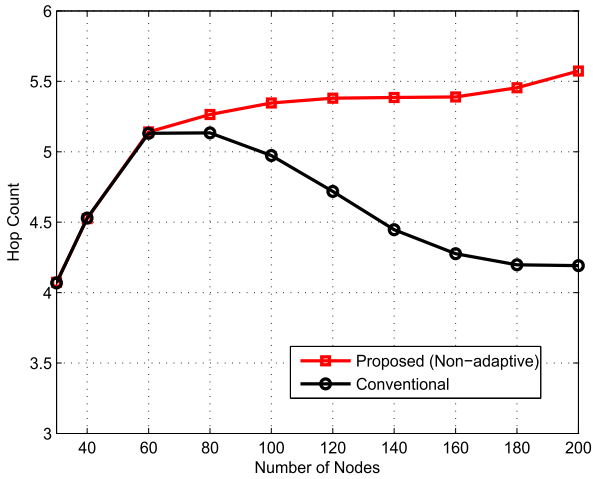


FIGURE 8. Hop count vs. number of nodes (number of nodes = 100, speed = 140~160 km/h, and keep time = 10 sec).

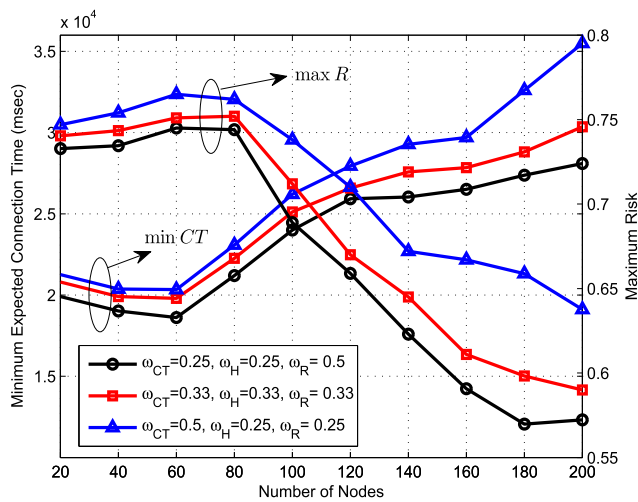


FIGURE 9. Minimum expected connection time and maximum risk vs. number of nodes (speed = 140~160 km/h, keep time = 10 sec).

In Fig. 9, we examine the minimum expected connection time and maximum risk value obtained for the proposed scheme when we vary weights ω_{CT} , ω_H , and ω_R while calculating the utility function. We can see that when we set ω_{CT} to 0.25, 0.33 and 0.5, the expected connection time decreases till the number of nodes reaches 60 and beyond that it increases. As explained in Fig. 8, since the flying nodes are not fully connected till number of nodes reaches to 60, with increasing trend in hop count, min CT decreases while the number of nodes is below 60. Beyond 60, flying nodes are fully connected and multiple intermediate nodes are available for selection, so the diversity in selection option also increases. As such, the minimum expected connection time increases when the number of nodes increases beyond 60. Conversely, maximum risk increases while the number of nodes is below 60 and finally starts decreasing when the number goes beyond 60. We can also see that as ω_{CT} increased from 0.25 to 0.33 and 0.5, the utility function gives higher priority to expected connection time of the selected link over

risk and hop count. This results in an increment in the minimum expected connection time. Similarly, when ω_R increase from 0.25 to 0.33 and 0.5, the utility function gives higher priority to the risk factor of the selected intermediate nodes over hop count and expected connection time. This ensures that risk value of the selected intermediate nodes is lowered.

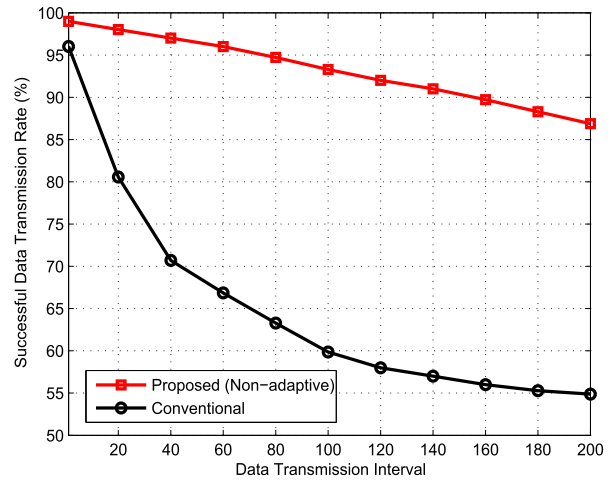


FIGURE 10. Successful data delivery ratio (number of nodes = 100, speed = 140~160 km/h, keep time = 10 sec).

In Fig. 10, we show a successful data delivery transmission rate versus data transmission interval for the proposed and conventional schemes. Data transmission interval refers to the regular time interval at which the source transmits data. We can see that the successful data transmission rate drastically degrades as the data transmission interval increases. The successful data transmission rate also decreases in our proposed scheme but the performance degradation rate is low. For instance, at a data transmission interval of 200msec, the successful transmission rate for the proposed scheme is approximately 87% while it is merely 55% for the conventional method.

In Fig. 11, we investigate the probability density function for the ratio of the actual path lifetime over the corresponding expected connection time for several values of keep time. If the ratio is smaller than 1, it signifies that the route link disconnected earlier than the expected connection time which may cause disruption during service. On the other hand, if the ratio is greater than 1, it signifies that route link exists for longer duration than expected connection time resulting no service disruption. We can see that with a lower value for keep time, the ratio is hardly less than 1. As the value of keep time increases, the probability of the ratio being less than 1 also increases. The mean value is found to be 2.02, 1.78, 1.42 and 1.26 for keep time 8, 10, 15 and 20 seconds respectively. Here, it should be noted that the larger keep time shortens the actual path lifetime, whereas a small keep time extends the actual average path lifetime. Also, the expected path lifetime is derived during the path setup procedure and selected UAVs for routing have the movement vector information from that time only. Therefore, the expected path lifetime is computed

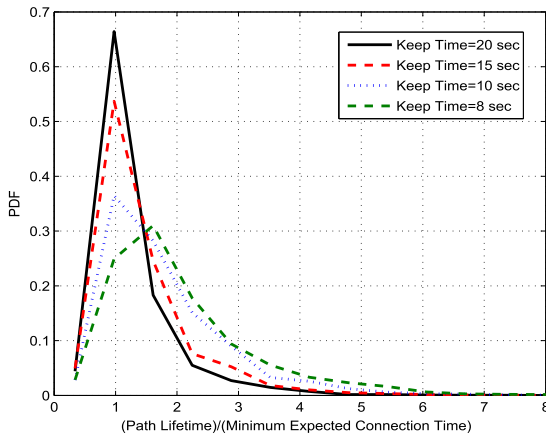


FIGURE 11. Probability density function for the ratio of path lifetime to minimum expected connection time.

on the assumption that UAVs move continuously with the current movement vectors which means keep time is assumed to be infinite. Furthermore, during the route setup time, only the initial fixed directional angle is assumed to derive the connection time. But, during DATA and ACK transmission, the proposed angle adjustment method is applied depending on the estimated UAV position of the neighboring UAVs, which helps to extend the actual path life time. With these effects, the actual average path life time can be generally longer than the expected path life i.e. expected connection time. This indicates that the proposed expected path life time is designed to prepare for the worst case scenario, and is determined in a conservative way. Therefore, we can find the majority of the distributed area under the curve beyond 1 indicating actual route link exists longer than expected connection time. Therefore, the our prediction mechanism for the expected connection time can sufficiently guarantee the existence of a link between nodes even at higher keep time.

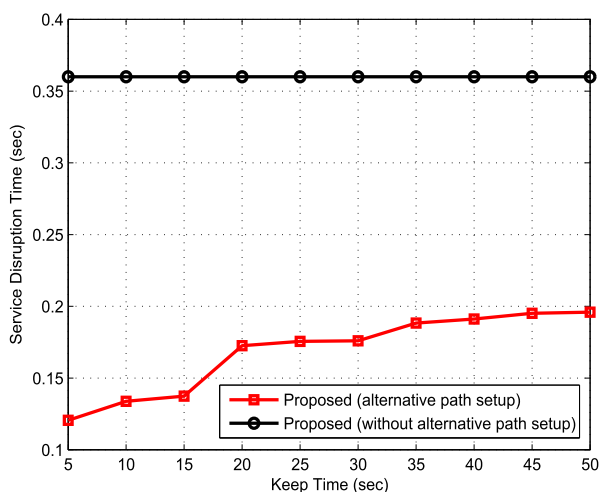


FIGURE 12. Service disruption time vs. keep time (number of nodes = 100, speed = 140~160 km/h).

In Fig. 12, we show service disruption time versus keep time for the proposed protocol with and without the

alternative path setup feature. We can see that service disruption time for the proposed protocol with the alternative path setup feature is considerably lower than without the alternative path setup feature even for higher values of keep time. Thus, we confirm that this feature helps further enhance the reliability of the proposed scheme.

V. CONCLUSIONS

In conclusion, we proposed a novel robust and reliable predictive routing scheme with directional and dynamic angle adjustment transmission for FANETS. Several new features of the proposed scheme were explained in detail such as prediction of the expected connection time, a utility function for path selection, directional transmission with a fresh update mechanism, dynamic angle adjustment with the use of an adaptive antenna, alternative path setup, and local path repair. A performance evaluation of the proposed scheme was carried out comparing it to the conventional scheme. The result showed that the proposed routing scheme increased the route setup success rate and the active-path lifetime. With the help of the dynamic angle adjustment transmission data delivery ratio, path lifetime and service disruption time also showed improvement, compared to static directional antenna transmission with a non-adaptive antenna.

REFERENCES

- [1] Z. Sun *et al.*, "BorderSense: Border patrol through advanced wireless sensor networks," *Ad Hoc Netw.*, vol. 9, no. 3, pp. 468–477, May 2011.
- [2] C. Barrado, R. Messeguer, J. Lopez, E. Pastor, E. Santamaria, and P. Royo, "Wildfire monitoring using a mixed air-ground mobile network," *IEEE Pervasive Comput.*, vol. 9, no. 4, pp. 24–32, Oct. 2010.
- [3] J. G. Manathara, P. B. Sujit, and R. W. Beard, "Multiple UAV coalitions for a search and prosecute mission," *J. Intell. Robot. Syst.*, vol. 62, no. 1, pp. 125–158, 2010.
- [4] I. Maza, F. Caballero, J. Capitan, J. R. Martinez-De-Dios, and A. Ollero, "Experimental results in multi-UAV coordination for disaster management and civil security applications," *J. Intell. Robot. Syst.*, vol. 61, nos. 1–4, pp. 563–585, 2011.
- [5] H. Xiang and L. Tian, "Development of a low-cost agricultural remote sensing system based on an autonomous unmanned aerial vehicle (UAV)," *Biosyst. Eng.*, vol. 108, no. 2, pp. 174–190, 2011.
- [6] W. Zafar and B. M. Khan, "Flying ad-hoc networks: Technological and social implications," *IEEE Technol. Soc. Mag.*, vol. 35, no. 2, pp. 67–74, Jun. 2016.
- [7] I. Bekmezci, O. K. Sahingoz, and Ş. Temel, "Flying ad-hoc networks (FANETS): A survey," *Ad Hoc Netw.*, vol. 11, no. 3, pp. 1254–1270, 2013.
- [8] E. W. Frew and T. X. Brown, "Networking issues for small unmanned aircraft systems," *J. Intell. Robot. Syst.*, vol. 54, no. 1, pp. 21–37, 2008.
- [9] O. K. Sahingoz, "Networking models in flying ad-hoc networks (FANETS): Concepts and challenges," *J. Intell. Robot. Syst.*, vol. 74, no. 1, pp. 512–527, 2014.
- [10] K. Singh and A. K. Verma, "Applying OLSR routing in FANETS," in *Proc. Int. Conf. Adv. Commun. Control Comput. Technol. (ICACCT)*, 2014, pp. 1212–1215.
- [11] K. Singh and A. K. Verma, "Experimental analysis of AODV, DSDV and OLSR routing protocol for flying ad-hoc networks (FANETS)," in *Proc. Int. Conf. Electr., Comput. Commun. Technol. (ICECCT)*, Mar. 2015, pp. 1–4.
- [12] S. Temel and I. Bekmezci, "LODMAC: Location oriented directional MAC protocol for FANETS," *Comput. Netw.*, vol. 83, pp. 76–84, Jun. 2015.
- [13] D. S. Vasiliev, A. Abilov, and V. V. Khrorenkov, "Peer selection algorithm in flying ad hoc networks," in *Proc. Int. Siberian Conf. Control Commun. (SIBCON)*, 2016, pp. 1–4.

- [14] A. V. Leonov, "Application of bee colony algorithm for FANET routing," in *Proc. Int. Conf. Young Specialist Micro/Nanotechnol. Electron Devices*, pp. 124–132, 2016.
- [15] V. A. Maistrenko, L. V. Alexey, and V. A. Danil, "Experimental estimate of using the ant colony optimization algorithm to solve the routing problem in FANET," in *Proc. Int. Conf. Control Commun. (SIBCON)*, 2016, pp. 1–4.
- [16] S. Rosati, K. Kruzelecki, G. Heitz, D. Floreano, and B. Rimoldi, "Dynamic routing for flying ad hoc networks," *IEEE Trans. Vehic. Tech.*, vol. 65, no. 3, pp. 1690–1700, Mar. 2016.
- [17] S. Say, N. Aomi, T. Ando, and S. Shimamoto, "Circularly multi-directional antenna arrays with spatial reuse based MAC for aerial sensor networks," in *Proc. IEEE Int. Conf. Communi. Workshop (ICCW)*, Jun. 2015, pp. 2225–2230.
- [18] C. Perkins, E. Belding-Royer and S. Das, *Ad Hoc On-Demand Distance Vector (AODV) Routing*, Tech. Rep. RFC 3561, Feb. 2003.
- [19] M. H. Tareque, M. S. Hossain, and M. Atiquzzaman, "On the routing in flying ad hoc networks," in *Proc. Federated Conf. Comput. Sci. Inf. Syst. (FedCSIS)*, Sep. 2015, pp. 1–9.
- [20] L. Lin, Q. Sun, S. Wang, and F. Yang, "A geographic mobility prediction routing protocol for ad hoc UAV network," in *Proc. IEEE Globecom Workshops*, Dec. 2012, pp. 1597–1602.



GANBAYAR GANKHUYAG received the B.S degree from the Mongolian University of Science and Technology, Ulaanbaatar, Mongolia, in 2009. He is currently working toward the M.S degree in information and communication engineering with Multimedia Network Laboratory, Inha University, Korea. His research interests include wireless communications and ad-hoc networks.



ANISH PRASAD SHRESTHA received the B.E. degree in electronics and communication engineering from the National College of Engineering, Tribhuvan University, Nepal, in 2006, the M.E. degree in information and communication engineering from Chosun University, South Korea, in 2010, and the Ph.D. degree in information and communication engineering from Inha University, South Korea, in 2015. He is currently a Post-Doctoral Fellow with the Multimedia Network Laboratory, Inha University. His research interests include wireless communications, statistical signal processing, cryptography and information security, computer networks, and machine learning.



SANG-JO YOO received the B.S. degree in electronic communication engineering from Hanyang University, Seoul, South Korea, in 1988, and the M.S. and Ph.D. degrees in electrical engineering from the Korea Advanced Institute of Science and Technology, in 1990 and 2000, respectively. From 1990 to 2001, he was a Member of Technical Staff with the Korea Telecom Research and Development Group, where he was involved in communication protocol conformance testing and network design fields. From 1994 to 1995 and from 2007 to 2008, he was a Guest Researcher with the National Institute Standards and Technology, USA. Since 2001, he has been with Inha University, where he is currently a Professor with the Information and Communication Engineering Department. His current research interests include cognitive radio network protocols, adhoc wireless network, MAC and routing protocol design, wireless network QoS, and wireless sensor networks.

...